

# BOUNDARY ELEMENT METHOD APPLIED TO THE LIFTING BODIES NEAR THE FREE SURFACE

Hassan Ghassemi<sup>1</sup>, Ahmad Reza Kohansal<sup>2</sup>

1- Associate professor, Faculty of Marine Technology, Amirkabir University of Technology

2- PhD Student, Faculty of Marine Technology, Amirkabir University of Technology

## Abstract

In this study, the boundary element method is formulated to evaluate hydrodynamic characteristics of bodies including free surface effect. The method is based on two equations, the perturbation potential boundary integral and the pressure Kutta condition, which are solved simultaneously. The method uses isoparametric elements for both quantity and geometric on the boundary. The method is first applied to two three-dimensional bodies (hydrofoil and vertical strut) of the NACA4412 profiles and symmetric Joukowski with 12% thickness. It is assumed that hydrofoil moves in constant speed. Some results of the pressure distribution, lift, wave-making drag and wave pattern are presented. It is shown that the computational results are in good agreement with the experimental measurements and other calculated values.

**Keywords:** Three-dimensional hydrofoil, Free surface, Pressure distribution, Lift and drag coefficients, Wave pattern

## Nomenclature

$AR$ : aspect ratio  
 $C$ : chord length  
 $C_P$ : pressure coefficient  
 $C_W$ : wave-making drag  
 $C_L$ : lift coefficient  
 $P$ : pressure  
 $L$ : lift  
 $R_W$ : wave-making resistance  
 $F_n$ : Froude number  
 $g$ : gravitational acceleration  
 $G$ : Green's function  
 $h$ : depth of the hydrofoil from free surface  
 $h/C$ : depth-chord ratio  
 $N_B$ : number of elements on the body  
 $N_F$ : number of elements on the free surface  
 $N_W$ : number of elements on the trailing vortex wake surface  
 $M$ : number and spanwise of the hydrofoil  
 $N_B$ : total number of the elements on the body

$N_F$ : total number of the elements on the free surface  
 $N_T$ : total number of element  
 $R_{pq}$ : distance between the singular point P and integration point Q  
 $R'_{pq}$ : distance between the singular point P and image integration point Q'  
 $\vec{V}_0$ : inflow velocity  
 $\vec{V}_t$ : induced velocity  
 $\vec{X}$ : position vector  
 $K_0$ : wave number  
 $\vec{n} = (n_x, n_y, n_z)$ : outward unit normal vector  
 $P_{TE}^{Back}$ : pressure at back side of TE  
 $P_{TE}^{FS}$ : pressure at face side of TE  
 $S$ : area of a body  
 $S_B$ : surface of the body  
 $S_F$ : surface of the free surface  
 $S_W$ : surface of the TVW  
 $DB_{ij}, SB_{ij}$ : influence coefficient of source, double on the body

$DW_{ij}$ ,  $SF_{ij}$ : influence coefficient of double  
and source on the wake and free surface  
 $\partial\phi/\partial n$ : normal derivative of the velocity  
potential  
 $\zeta$ : wave elevation  
 $\phi$ : perturbation potential  
 $\Phi$ : total velocity potential  
 $\phi_{in}$ : free stream velocity potential  
 $\phi_z$ : first derivative of the potential in z-  
direction  
 $\phi_{xx}$ : second derivative of the potential in  
x-direction  
 $\delta_{ij}$ : Kronecker delta function  
 $\sigma$ : source strength on each free surface  
element  
 $\rho$ : density of the water  
 $\alpha$ : attack angle  
 $\Delta\phi$ : difference of the velocity potential  
at TE

## 1. Introduction

Lifting bodies like hydrofoils are widely used in ships and marine vehicles. Hydrofoils are used to decrease resistance and increase lift and speed for many crafts. The prediction of hydrodynamic characteristics of hydrofoils plays an important role in the design of these crafts.

When a lifting body moves near the free surface, its flow field and consequently wave pattern will be changed and predictions of hydrodynamic characteristics are more complicate. In this situation, the effect of the free surface on the wave profile, pressure distribution, lift and resistance should be considered.

This problem has been conducted by many researchers. Bal [1] used the potential based panel method for 2-D hydrofoil. Yeung and Bouger [2] dealt with thick foil methods which provided a precise representation of the flow near the hydrofoil surface. Janson [3] applied linear and nonlinear potential flow

calculations of free surface waves including lift and induced drag of hydrofoils, vertical struts and Wigley ship hull. Larson and Janson [4] developed a three-dimensional panel method for yacht potential flow simulation. In their method, source and doublet are distributed on the lifting part of yacht. There have been some experimental as well as theoretical studies on influence of different foil configurations on the hydrodynamic characteristics [5]. Hydrodynamic analysis of two and three dimensional hydrofoils moving beneath the free surface was developed in [6] and [7]. Bai and Han [8] used a localized finite-element method for the nonlinear steady waves due to two-dimensional hydrofoils. Numerical calculations of ship induced waves using boundary element method with triangular mesh surface calculated by Sadathosseini et al. in [9]. Dawson [10] employed a distribution of Rankine type of sources on the ship hull and free surface. Recently, Ghassemi and Kohansal [11] presented nonlinear free surface flow and higher order boundary element method on the various submerged and surface body.

In the present study, the boundary element method is developed to predict the free surface effect over two and three-dimensional hydrofoils moving near it. Also this method is used to calculate the hydrodynamic characteristics of surface piercing bodies. The surfaces are discretized into several quadrilateral elements. The pressure distribution, lift and wave making resistance coefficients on the hydrofoil surface are obtained in various Froude number, angle of attack, depth of submergence and aspect ratio. In addition, the wave pattern due to moving hydrofoil is predicted. Finally, numerical

results are compared with experimental data, which reveal good agreement.

## 2. Mathematical method

Consider a Cartesian coordinate system fixed in the space  $O-XYZ$  and a moving coordinate system fixed on the hydrofoil  $o-xyz$ . The horizontal and vertical axes,  $ox$  and  $oz$ , are along and at the right angle to the direction of the motion. The body-fixed coordinate system  $oxyz$  moves with constant speed,  $V_0$ , in the  $x$ -direction.

The hydrofoil travels at a constant forward speed,  $V_0$ , in a calm water surface and unrestricted flow. The fluid is assumed to be inviscid, incompressible and without surface tension, and flow to be irrotational. These assumptions lead to a boundary value problem for the velocity potential with the Laplace equation satisfied in the fluid. Under the global coordinate system, a total velocity potential  $\Phi$  can be defined as follows:

$$\Phi = \phi + \vec{V}_0 \cdot \vec{X}, \quad (1)$$

where  $\phi$  is the perturbation velocity potential.

The perturbation potential is governed by Laplace's equation:

$$\nabla^2 \phi = 0, \quad (2)$$

The potential  $\phi$  is computed by the boundary element method, which is based on the Green's identity. In general, the boundary surface includes the body surface ( $S_B$ ), wake surface ( $S_W$ ) and the free surface ( $S_{FS}$ ). According to Green's third identity, the perturbation potential  $\phi$  is given by the following integral expression with points  $Q$  on surface  $S$  and  $P$  in  $D$ :

$$4\pi E \phi(P) = \int_S \left[ \frac{\partial \phi(Q)}{\partial n} G - \phi(Q) \frac{\partial G}{\partial n} \right] dS, \quad (3)$$

where  $S = S_B + S_W + S_{FS}$  are the boundaries of the lifting body, wake and the free surface, respectively.  $P$  is the field point and  $E$  is the solid angle which depends on its position in the fluid domain  $D$ . If point  $P$  is placed on the boundary (body surface), then the coefficient  $E$  is replaced by  $1/2$ . For  $P$  inside and outside  $D$ , its values are one and zero, respectively.  $G$  is the Green's function including image body relative to the free surface.

$$G = \frac{1}{R_{pq}} + \frac{1}{R'_{pq}} \quad (4)$$

where  $R_{pq}$  is the magnitude of the vector from point  $q$  to  $p$  and  $R'_{pq}$  is the magnitude of the vector from image of point  $q'$  to  $p$ .

$$\begin{cases} R_{pq} = \sqrt{(x-\xi)^2 + (y-\eta)^2 + (z-\zeta)^2} \\ R'_{pq} = \sqrt{(x-\xi')^2 + (y-\eta')^2 + (z+\zeta')^2} \end{cases} \quad (5)$$

Boundary conditions are given as follows:

**i) On the body surface:** It states that derivative of the total potential velocity normal to body surface is zero. Using Eq. (1), we obtain

$$\frac{\partial \Phi}{\partial n} = 0 \Rightarrow \frac{\partial \phi}{\partial n} = -\vec{V}_0 \cdot \vec{n} \quad (6)$$

**ii). On the free surface:**

$$(\nabla \phi - \vec{V}_0) \cdot \nabla \zeta = \phi_z \quad \text{on } z = \zeta(x, y), \quad (7)$$

where  $\zeta$  wave elevation is

$$\zeta = \frac{1}{g} \left( -\vec{V}_0 \cdot \nabla \phi + \frac{1}{2} \nabla \phi \cdot \nabla \phi \right), \quad (8)$$

on  $z = \zeta(x, y)$ ,

**iii). At infinity:**

$$\lim |\nabla \phi| = 0, \quad \text{when } r \rightarrow \infty, \quad (9)$$

**iv). Kutta Condition at trailing edge:** The separation of the flow corresponds to the flow at the trailing edge on classical airfoil theory and is secured through the Kutta condition. In the other word, the velocity should be finite at the Trailing edge (TE).

$$|\nabla \phi| < \infty \quad \text{at TE on Foil} \quad (10)$$

Numerically, the Kutta condition expresses that the pressure is equal at the TE. It means

$$\Delta P_{TE} = 0 \Rightarrow P_{TE}^{Back} - P_{TE}^{Face} = 0 \quad (11)$$

The free surface formulation (Eq. (8)) is nonlinear. Here, the linearized boundary-value problem is used by omitting the nonlinear terms in the boundary conditions. Then, the linearized boundary conditions are satisfied on the undisturbed free surface

$$-V_0 \zeta = \phi_z \quad \text{on } z = 0, \quad (12)$$

$$\zeta = -\frac{1}{g} V_0 \phi_x \quad \text{on } z = 0, \quad (13)$$

Substituting Eq. (12) into Eq. (13), a composed boundary condition on the free surface is obtained:

$$V_0^2 \phi_{xx} = g \phi_z \quad \text{on } z = 0, \quad (14)$$

### 3. Numerical method

The body surface and free surface are discretized into the quadrilateral elements. The discretized form of integral Eq. (3) for the wetted body surface and free surface are expressed as

$$\sum_{j=1}^{N_B} [\delta_{ij} - DB_{ij}] - \sum_{j=1}^{N_B} [SB_{ij}] + \sum_{j=1}^{N_F} [SF_{ij}] = 0, \quad i = 1, 2, \dots, N_B \quad (15)$$

$$\sum_{j=1}^{N_B} \frac{\partial^2 [DB_{ij}]}{\partial x^2} - \sum_{j=1}^{N_B} \frac{\partial^2 [SB_{ij}]}{\partial x^2} + \sum_{j=1}^{N_F} \left( \frac{\partial^2 [SF_{ij}]}{\partial x^2} - K_0 \delta_{ij} \right) = 0, \quad i = 1, 2, \dots, N_F \quad (16)$$

Where

$$\begin{cases} DB_{ij} = \frac{1}{4\pi E} \int_{S_B} \phi_j \frac{\partial G_{ij}}{\partial n} dS_j, \\ SB_{ij} = \frac{1}{4\pi E} \int_{S_B} (\partial \phi / \partial n)_j G_{ij} dS_j, \\ SF_{ij} = \frac{1}{4\pi E} \int_{S_F} (\partial \phi / \partial n)_j \frac{1}{r_{ij}} dS_j, \end{cases} \quad (17)$$

and  $N_B$  and  $N_F$  are the number of elements on the body and free surfaces, respectively. The velocity component  $(\partial \phi / \partial n)_j$  and potential  $\phi_j$  on the  $j$ -th element can be expressed as

$$\begin{cases} (\partial \phi / \partial n)_F = \sigma_j + \frac{\partial \sigma_j}{\partial \xi} \xi + \frac{\partial \sigma_j}{\partial \eta} \eta \\ (\partial \phi / \partial n)_B = \text{is known from Eq. (6).} \\ \phi(\xi, \eta) = \phi_j + \frac{\partial \phi_j}{\partial \xi} \xi + \frac{\partial \phi_j}{\partial \eta} \eta \end{cases} \quad (18)$$

where  $\delta_{ij}$  is Kronecker delta function. The total numbers of unknowns are  $N_B + N_F (= N_T)$ .  $N_B$  is the number of potential ( $\phi$ ) on the body surface, and  $N_F$  is the number of velocity components ( $\sigma$ ) on the free surface. The matrix form of combined equations (15) and (16) are expressed as

$$\begin{bmatrix} [\delta - DB]_{N_B \times N_B} & [SF]_{N_B \times N_F} \\ [DB]_{N_F \times N_B} & [-K_0 \delta + SF]_{N_F \times N_F} \end{bmatrix} \begin{Bmatrix} \{\phi\}_{N_B \times 1} \\ \{\sigma\}_{N_F \times 1} \end{Bmatrix} = \begin{bmatrix} [SB]_{N_B \times N_B} & [0]_{N_B \times N_F} \\ [SB]_{N_F \times N_B} & [0]_{N_F \times N_F} \end{bmatrix} \begin{Bmatrix} \{-\vec{V}_h \cdot \vec{n}\}_{N_B \times 1} \\ \{0\}_{N_F \times 1} \end{Bmatrix} \quad (19)$$

Here, the second derivative of the influence coefficients ( $DB_{xx}$ ,  $SB_{xx}$ ,  $SF_{xx}$ ) is computed by the four-point finite difference operator, and also the four-point upstream operator is introduced to satisfy the condition of no waves propagating upstream.

Another matrix form of equation (19) is

$$[A]_{N_T \times N_T} \{x\}_{N_T \times 1} = \{b\}_{N_T \times 1}, \quad (20)$$

For this type of problem, a formal solution may be given by the direct solution methods of *LU* decomposition or Gaussian elimination. However, the solution vector may have extensively large components whose algebraic elimination, when multiplied by the matrix  $A$ , may give a poor approximation for the right-hand vector  $b$ . This affects the errors in the solution of the matrix Eq. (20). In the present study, singular value decomposition (SVD) technique has been adopted to solve matrix Eq. (20).

Once the perturbation potential is obtained, the induced velocity may be determined by the derivative of the perturbation potential,  $\bar{v}_i = \nabla \phi$ . The pressure and its dimensionless coefficient on the hydrofoil surface are calculated by

$$P = 0.5\rho(2V_0.v_t - v_t^2), \quad (21)$$

The hydrodynamic forces (lift and wave-making drag) acting on the hydrofoil can be obtained by integrating the pressure over the surface

$$L = \rho \int_{S_B} \left( \frac{1}{2} \nabla \phi \cdot \nabla \phi - \frac{1}{2} V_0^2 \right) n_z dS \quad (22)$$

$$R_w = \rho \int_{S_B} \left( \frac{1}{2} \nabla \phi \cdot \nabla \phi - \frac{1}{2} V_0^2 \right) n_x dS \quad (23)$$

where  $\vec{n}(n_x, n_y, n_z)$  is outward unit normal vector on the hydrofoil.

Finally, non-dimensional parameters (pressure, lift, wave-making drag) are calculated by

$$\begin{cases} C_p = \frac{P}{0.5\rho V_0^2}, \\ C_w = \frac{R_w}{0.5\rho V_0^2 S} \\ C_L = \frac{L}{0.5\rho V_0^2 S} \end{cases} \quad (24)$$

and wave elevation is expressed as

$$\xi = -\frac{V_0}{g} \frac{\partial \phi}{\partial x} \quad \text{on} \quad S_F \quad (25)$$

#### 4. Numerical calculations

A three-dimensional hydrofoil with NACA4412 and symmetric Joukowski ( $t/C = 0.12$ ) profiles are chosen in order to compare present numerical results with the experimental measurements in various conditions. For Joukowski hydrofoil, the aspect ratio (*square span/planform area*) is considered 10 since the results can be compared with those of available experimental data and numerical results of other researchers. The body is discretized into 15 strips in spanwise and 30 strips in chord-wise direction. So, numbers of elements on the foil and on the free surface are 900 and 3600, respectively, which totally become 4500 elements.

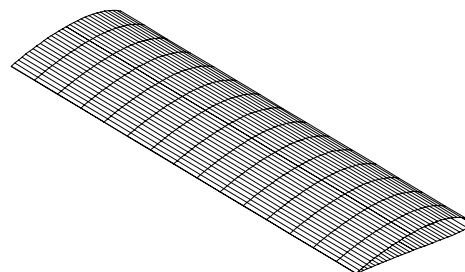


Fig. 1- Surface mesh of the rectangular hydrofoil NACA4412,  $AR = 6$  (Number of elements =  $N_{Tot} = 900$ )

A three dimensional hydrofoil with NACA4412 has a non-symmetric profile and we focused on this to compute more results by present method. Figure 1 shows the surface mesh of the NACA4412 foil and aspect ratio ( $AR=6$ ). In Figure 2, for this foil at depth ratio ( $h/C=1$ ), attack angle ( $\alpha = 5[\text{deg.}]$ ) and Froude number ( $F_n = 1$ ), the computational results of the center plane wave profile are compared with calculated values given by Kouh et. al. (2002) and Xie and Vassalos (2007). The velocity potential and pressure distribution on the NACA4412 foil are shown in Figures 3 and 4 at  $AR=10$ ,  $\alpha = 5[\text{deg.}]$  and  $h/C=1$ . The pressure distribution is compared with Yeung and Bouger numerical results. Good agreement is reached with 2D results between the present computational results and other numerical and experimental data.

A comparison of lift and wave-making drag coefficients versus Froude number are shown in Figures 5 and 6, respectively. Figures 7 and 8 show lift and wave-making drag versus foil immersion depth ratio at three Froude numbers ( $F_n = 0.7, 1.0$  and  $1.5$ ), respectively. As indicated in these Figures, the effect of the free surface is that it increases the lift coefficient for Froude number up to almost 0.5. The lift coefficient is then diminished as the speed increases. This is also almost the same for the wave-making drag but the hump condition is shown at Froude number 0.8.

It can be seen that the effect of immersion on the hydrodynamic performance is significant when the foil is located near the free surface. Figure 9 shows the lift for the foils with three aspect ratios of  $AR=4, 5$  and  $6$ . The immersion depth is  $h/C=1$ . The lift

coefficients decrease as the aspect ratio decreases.

Figure 10 shows the present computational results and experimental data (measured by Bai and Han, 1994) of pressure distribution on symmetric Joukowski hydrofoil. The Froude number is  $F_n = 0.95$  and is immersed at two depth ratio 1 and 1.8, ( $h/C = 1.8, h/C = 1.0$ ). Chord length Froude number is defined as  $F_n = V_0 / \sqrt{C \cdot g}$ , where  $C$  is chord length. The present results are given at mid-span of the foil. This figure shows clearly the effect of  $h/c$  on the flow characteristics over this hydrofoil.

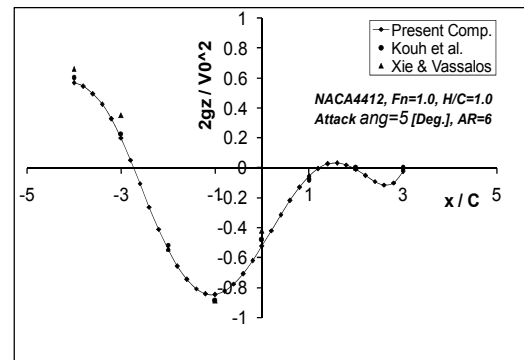


Fig. 2- Comparison of wave profile at the center plane of NACA4412 foil

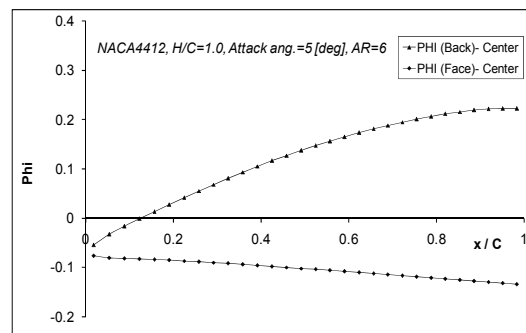


Fig. 3- Potential distribution on the NACA4412 foil,  $AR = 10$ ,  $\alpha = 5[\text{deg.}]$

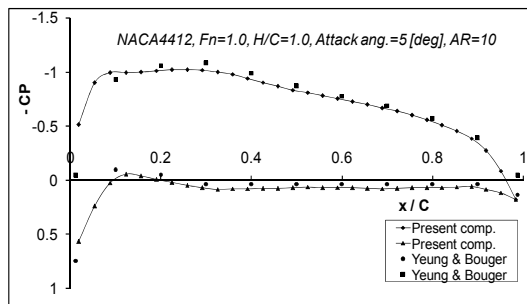


Fig. 4- Comparison of pressure distribution on the NACA4412 foil,  $AR = 10$ ,  $\alpha = 5[deg.]$

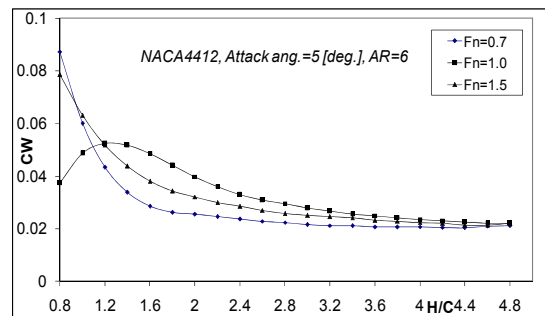


Fig. 8- Wave-making resistance coefficients versus immersion depth at three Froude number (NACA4412)

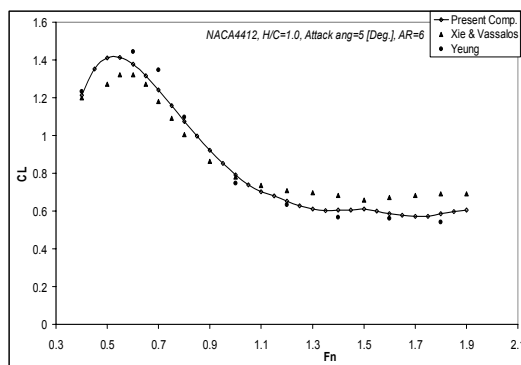


Fig. 5- Comparison of lift coefficient of NACA4412 at center plane

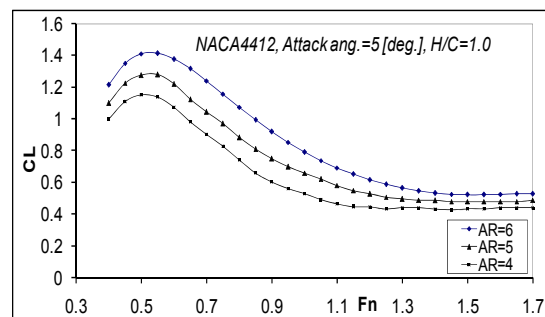


Fig. 9- Lift coefficients versus Froude numbers at various aspect ratios (NACA4412)

Wave pattern of the hydrofoils are calculated by the present method in various conditions. Figure 11 shows wave pattern on the Joukowski hydrofoil at  $h/C = 0.3$ ,  $AR = 3$ ,  $\alpha = 5[deg.]$ ,  $Fn = 0.7$ .

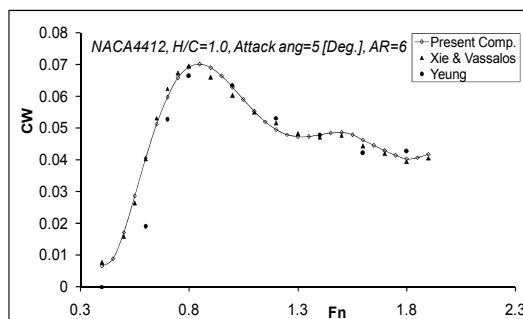


Fig. 6- Comparison of wave-making drag coefficient of NACA4412 at center plane

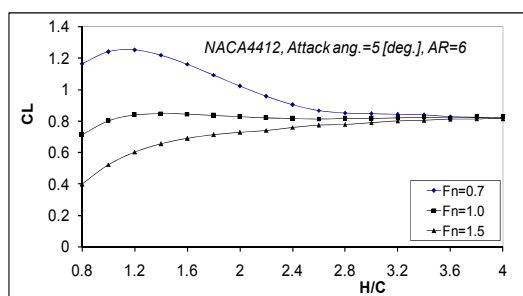


Fig. 7- Lift coefficients versus immersion depth at three Froude numbers (NACA4412)

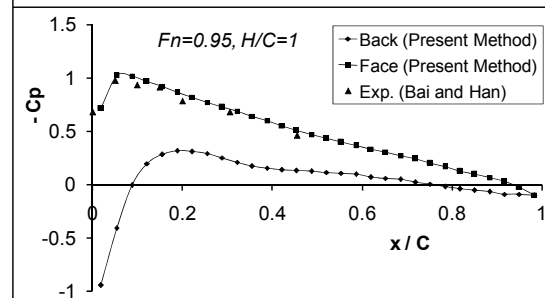
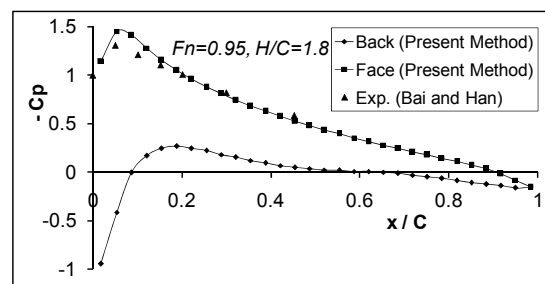
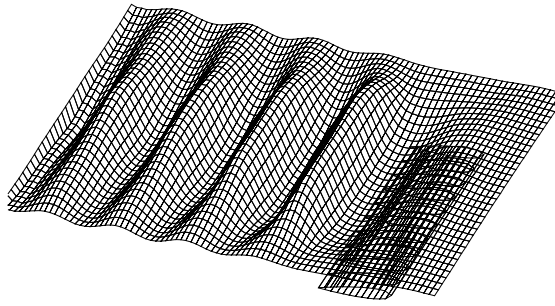
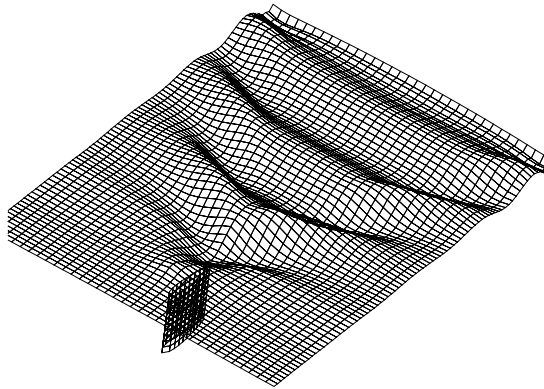


Fig. 10- Comparison of the pressure distribution on symmetric Joukowski hydrofoil,  $AR = 10$ ,  $\alpha = 5[deg.]$



**Fig. 11- Wave pattern on the Joukowski profile**  $h/C = 0.3$ ,  $AR = 3$ ,  $\alpha = 5[\text{deg.}]$ ,  
 $F_n = 0.7$



**Fig. 12- wave pattern on vertical strut Joukowski profile,**  $h/C = 0.3$ ,  
 $AR = 1$ ,  $F_n = 0.5$

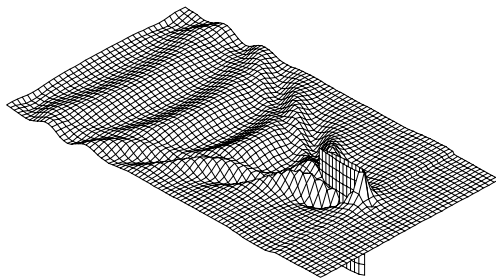


**Fig. 13- Wave pattern on vertical strut Joukowski profile,**  $AR = 2$ ,  $F_n = 0.5$

Also hydrodynamic characteristics of surface piercing bodies like vertical struts are resulted from this method. For example wave pattern on vertical strut of Joukowski profile, at  $AR = 2$  and

$F_n = 0.5$  and two different submergence depth are represented in Figures 12 and 13.

## 5. Conclusion

This paper used the boundary element method for the lifting bodies near the free surface. The hydrodynamic characteristics of the two hydrofoil profiles were investigated in terms of various aspect ratios, Froude numbers and depth ratios. By comparing the results of pressure distribution, lift, drag and wave elevation with those of experiments and other numerical values, it is revealed that the method is accurate and efficient. In addition it is clear that when submergence of a body becomes small, effect of free surface should be considered. It is shown that high precision can be achieved by taking smaller elements on some regions where the flow changes rapidly. Also it is revealed that the method can accurately predict the hydrodynamic characteristics of surface piercing bodies.

## 6. References

- 1-Bal S., (1999): "A potential based panel method for 2-D hydrofoil", Ocean Engineering Vol. 26, pp.343-361
- 2-Yeung R. W., Bouger Y. C., (1979): "A hybrid-integral equation method for steady two-dimensional ship waves", Int. J. Num. Meth. Engng. (14), 317-336.
- 3-Janson, C.E., (1997): "potential flow panel method for the calculation of free surface flows with lift", PhD dissertation, Chalmers university of Technology,
- 4-Larson ,L. Janson C.E. (1999): "Potential flow calculations for sailing yachts", CFD for Ship and Offshore Design, 31<sup>st</sup> WEGMENT School, Hamburg.
- 5-Kouh J. S., (2002): "Performance analysis of two dimensional hydrofoil under free surface", Journal of National Taiwan University 86.
- 6-Xie N., Vassalos D. (2007): "Performance analysis of 3D hydrofoil under free surface", Ocean Engineering Vol. 34, pp. 1257–1264.



- 7-Teles da Silva, A. F. and Peregrine, D. H. (1990): "Nonlinear perturbations on a free surface induced by a submerged body: a boundary integral approach", *Engineering Analysis with Boundary Elements*, 7(4), 214-222.
- 8-Bai, K.J., Han, J.H., (1994): "A localized finite-element method for the nonlinear steady waves due to a two-dimensional hydrofoil", *J. Ship Res.* 38, 42–51.
- 9-Sadathosseini S.H., Mousaviraad S.M., Seif M.S., (2003): "Numerical calculations of ship induced waves", *Journal of Marine Engineering*, Vol.1, No.2.
- 10-Dawson, C. W., (1977): "A practical computer method for solving ship-wave problems", *Proceedings of Second International Conference on Numerical Ship Hydrodynamics*, pp. 30-38.
- 11-Ghassemi, H., Kohansal, A.R., (2009) Higher order boundary element method applied to the hydrofoil beneath the free surface, *Proceedings of the 28<sup>th</sup> International Conference on OMAE*, Hawaii, USA.